Carbon 126 (2018) 419–425

Contents lists available at ScienceDirect

Carbon

journal homepage: www.elsevier.com/locate/carbon

Highly flexible and shape-persistent graphene microtube and its application in supercapacitor

Junjie Yang, Wei Weng**, Yang Zhang, Xiaowen Du, Yunxia Liang, Lijun Yang, Xiaogang Luo, Yanhua Cheng, Meifang Zhu*

State Key Laboratory for Modification of Chemical Fibers and Polymer Materials, College of Materials Science and Engineering, Donghua University, Shanghai 201620, China

ARTICLE INFO

Article history:
Received 6 July 2017
Received in revised form
14 September 2017
Accepted 14 October 2017
Available online 15 October 2017

ABSTRACT

Graphene microtube has a robust potential application in gas separation, catalysis, water treatment and electronics. At present it remains two big challenges: high persistence of the tubular structure and high quality of the microtube. Here, a novel electrochemical technique was proposed, in which graphene oxides can be simultaneously deposited and reduced on a template wire at room temperature. After removing the template, the tubular structure was formed and complied well with the shape of the template. Moreover, the tube wall is composed of highly aligned graphene sheets. These combined characters bring about excellent flexibility and electrochemical properties, e.g., the specific capacitance of the graphene microtube is 2.5 times the value of the graphene fiber with the same sectional area.

1. Introduction

Graphene, a two-dimensional carbon nanomaterial, has attracted much attention due to its extraordinary properties in mechanical, thermal, electrical and optical fields [1–3]. A single-layer graphene sheet with a thickness of 0.34 nm and a length or width of several to dozens of microns finds an application after assembled into a macro structure. To this end, various structures have been developed, e.g., film, sponge, ribbon, fiber and microtube [4–7]. Among them, graphene microtube is an emerging member. Since carbon tube has shown a great potential in gas separation, catalysis, water treatment and electronics, graphene microtube, an analogue of carbon tube, will prevail in these fields [8–12].

So far several methods have been developed to generate the graphene microtube, e.g., chemical vapor deposition (CVD) [13,14], hydrothermal synthesis [15] and wet-spinning [11]. However, these methods feature some disadvantages. In a typical CVD protocol, graphene was grown on a Cu wire under a super-high temperature of 1000 °C. When removing the Cu wire, the resulting tubular structure collapsed and it therefore failed to maintain its shape [14]. For the other two methods, graphene oxides (GO) were used as the starting material and the microtubes were reported to be shape-persistent, however with a low quality. They require long heat treatment time, for instance 2.5 h at 230 °C, or hazardous reducing agents to improve the quality [11,15]. The disadvantages of the available methods arouse a pressing need for an efficient and facile method towards shape-persistent and high-quality graphene microtube.

As for the use of the graphene microtube, a great potential is to construct exquisite fiber-shaped supercapacitors, which have been deemed as a promising energy storage device for the thriving flexible and wearable electronics [16–19]. They prevail over film-shaped and bulk supercapacitors in flexibility, wearability and scalable connection [20,21]. However, to the best of our knowledge the energy storage performance of the graphene microtube has not been unveiled to date. The main reason may be the poor quality of the existing graphene microtubes.

Herein, a novel electrochemical technique was proposed. GO could be simultaneously deposited and reduced on a Cu wire. After etching the Cu wire the tubular structure was retained, resulting in the graphene microtube. The method has several merits: short preparation time (e.g., 20 min), low temperatures (e.g., at room temperature) and environmental benignity. Moreover, the achieved graphene microtube is shape-persistent and possesses a high quality derived from the highly aligned graphene sheets in the tube wall. Consequently, it presents excellent flexibility and electrochemical performance. The graphene microtube maintains stable

* Corresponding author.
** Corresponding author.
E-mail addresses: gotovic@163.com (W. Weng), zhumf@dhu.edu.cn (M. Zhu).

https://doi.org/10.1016/j.carbon.2017.10.045
0008-6223/

under bending with an angle of 50° and has a large gravimetric specific capacitance of 135.5 F g^{-1}, which is 2.5 times the value of the graphene fiber with the same sectional area.

2. Experimental section

2.1. Preparation of graphene microtube (ERGO)

Graphene oxides (GO) were synthesized by a modified Hummers' method [22]. 1.0 wt% GO suspension of 85 ml was prepared by ultrasonic treatment for 20 min, afterwards adding 85 ml of 0.2 M lithium perchlorate aqueous solution under stirring, resulting in the plating solution. Cu wires with a diameter of 0.1 mm were washed by 1 M HCl solution, deionized water and ethanol successively, and then dried in the air. A three-electrode system was carried out to electrochemically grow the graphene microtube. The Cu wire, Pt wire served as the working and counter electrodes, respectively, together with the Ag/AgCl reference electrode. A constant potential mode was applied, i.e., the potential was kept at −1 V. The growth time was varied from 5 min to 60 min. The plating solution was kept at room temperature (25 °C) and stirred smoothly. When the growth ended, the graphene-coated Cu wire was immersed into 2 M $FeCl_3$ aqueous solution to etch the Cu wire, then washed with deionized water and dried in the air resulting in the graphene microtube.

2.2. Preparation of GO fiber and chemical reduced GO (CRGO) fiber

GO suspension with a concentration of 10 mg ml^{-1} was made by ultrasonic treatment for 20 min. Then the dispersion was heated to evaporate the water to achieve a high concentration of 40 mg ml^{-1} in 60 °C water bath. Continuous wet-spinning was carried out with a homemade spinning machine [23]. The GO dispersion was loaded into a plastic syringe and then injected into a rotating coagulation bath resulting in a gel fiber, which was rolled onto a drum and dried at 60 °C in vacuum leading to a GO fiber. Finally, the GO fiber was reduced by hydriodic acid (45%, Sinopharm) at 95 °C for 8 h followed by washing with deionized water thoroughly and drying at 80 °C for 12 h in vacuum.

2.3. Characterization

The structure and morphology of graphene microtubes were characterized by scanning electron microscope (SEM, Hitachi, SU8010). The composition and bonds were studied by Raman spectroscopy (Renishaw microRaman, 514.5 nm laser) and X-ray photoelectron spectroscopy (XPS, Thermo, Escalab 250). The weight of microtubes was measured by an ultra-microbalance (Mettler Toledo, XP6). The sheet resistance of graphene microtubes was tested by four-point probe (SX1944) and their conductivity was investigated by electrometer (Keithley, 6517B). The specific surface area and the pore diameter distribution were measured using the Brenauer-Emmett-Teller (BET) method by a surface area and porosity system (Micromeritics, ASAP2460) at 77 K.

2.4. Fabrication of all-solid-state supercapacitors and electrochemical measurements

Electrochemical workstation (Chenhua, CHI 660E) was used to investigate the electrochemical properties. A gel electrolyte was prepared. First, deionized water (10 ml) was mixed with phosphoric acid (10 mL) and stirred for 30 min. Second, PVA powder (1788, 10 g) was dissolved in 90 mL deionized water at 90 °C and then added to the above solution under stirring for 1 h, followed by cooling to the room temperature. A symmetrical two-electrode system was utilized. Two graphene microtubes were placed in parallel and separated by the gel electrolyte leading to a fiber-shaped supercapacitor. The current density was varied from 0.1 to 10 A g^{-1}. The voltage window was in a range of 0–0.8 V. The capacitance of the graphene microtubes was calculated from the galvanostatic charge/discharge curves, using the following equation:

$$C = (2 \times I \times \Delta t)/\Delta U$$

where I, Δt and ΔU correspond to the discharge current, discharge time and voltage window, respectively. The gravimetric specific capacitance (C_m) was computed from dividing C by the mass, which here is based on one graphene microtube, i.e., single electrode. To test the flexible performance, the fiber-shaped supercapacitor was fixed on a PET substrate and the electrochemical property was monitored when bending the substrate.

3. Results and discussion

Fig. 1 represents the preparation scheme of the electrochemically grown graphene microtube. GO was simultaneously deposited and reduced on the Cu wire driven by a protonation process under an electric field. After etching the Cu wire the graphene microtube was finally obtained. From the cyclic voltammograms (Fig. S1a) in a potential range from −0.4 to −1.5 V (vs. Ag/AgCl), a large cathodic current peak occurs at −1.2 V with a starting potential of −0.8 V. This large reduction current is ascribed to the reduction of the surface oxygen groups of GO since the reduction of water to hydrogen occurs at more negative potentials (e.g., nearly −1.5 V) [24]. Also from the Amperometric i-t curve at a constant potential of −1 V (Fig. S1b), the cathodic current decreased when extending the growth time, which indicates an increasingly inefficient reduction. Thus the growth time will affect the wall thickness of the microtube. From optical images (Fig. S2), the color of Cu wire was changed from golden yellow to dark after a short growth time, which verifies the graphene coating.

The architecture of graphene microtubes can be helical (Fig. 2a) or straight (Fig. 2b) corresponding to the shape of Cu wire. A characterized wavy surface was found for the graphene microtubes (Fig. 2c–e), which was caused by the wrinkling of the graphene sheets. The cross-sectional morphologies of the graphene microtubes with different growth time are shown in Fig. 2f–m. A hollow tubular structure is evident for all cases. And the inner diameters are complied with that of the Cu wire. More interestingly, a distinct layer-by-layer structure of the graphene sheets in the tube wall was formed (Fig. 2j, k, 2l and 2m), which indicates a high alignment of the graphene sheets. This could be beneficial for the properties of the graphene microtubes.

The wall thickness of the microtubes decreased after an initial increase when increasing the growth time and a maximum value was reached at the growth time of 20 min. Specifically, they are 1.2 μm, 1.9 μm, 1.3 μm and 1.0 μm according to the growth time of 10 min, 20 min, 30 min and 60 min, respectively. This trend was proofed by the mass of graphene microtubes (Fig. S3). Specifically, the dependence of the mass of graphene microtubes on the growth time was investigated. A maximum mass of 26 μg cm^{-1} was achieved at the growth time of 20 min. To have a deep probe, XPS tests were carried out for the reduced graphene oxides (rGO) on the Cu wire with different growth time, which were free of the following processes, e.g., etching the Cu wire and water washing (Fig. S4). And the concentrations of O element were listed in Table S1, i.e., 21.5%, 19.8%, 37.6% and 44.2% for the growth time of 10 min, 20 min, 30min and 60 min, respectively. The result is consistent with the

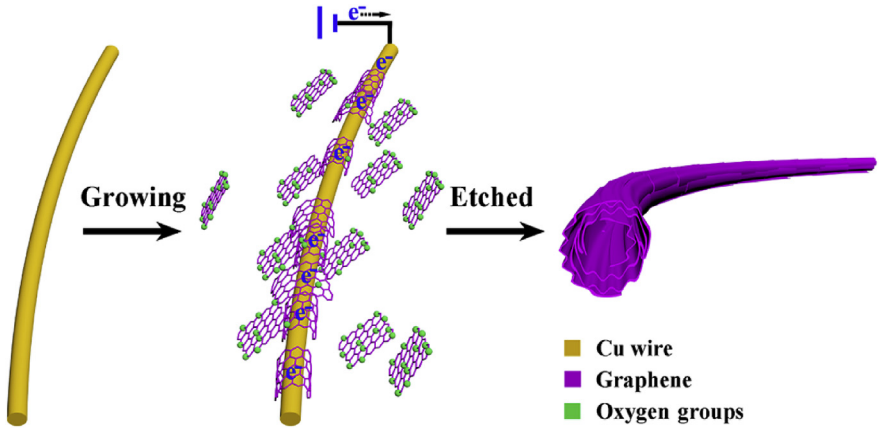

Fig. 1. Preparation scheme of the electrochemically grown graphene microtube. (A colour version of this figure can be viewed online.)

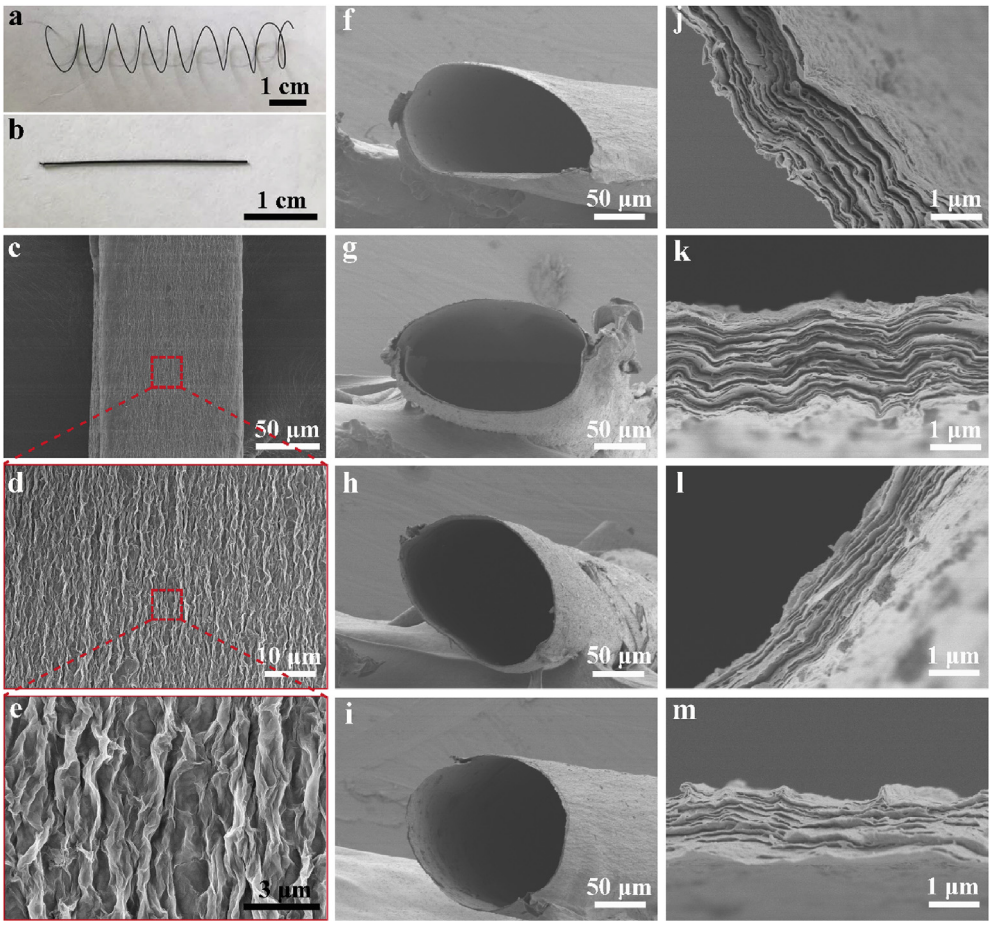

Fig. 2. Helical (**a**) and straight (**b**) graphene microtubes. Surface morphologies of the graphene microtubes with low (**c**), medium (**d**) and high (**e**) magnifications. Cross-sectional images of the graphene microtubes with the growth time of 10 min (**f** and **j**), 20 min (**g** and **k**), 30 min (**h** and **l**) and 60 min (**i** and **m**). (A colour version of this figure can be viewed online.)

dependence of cathodic current on the growth time (Fig. S1b). Therefore, the reason may lie in the decreasing efficiency of GO reduction with the increasing growth time and consequently these rGO with high oxygen concentrations can be detached in the water in the following processes. As a result, there exists an optimum growth time corresponding to a maximum wall thickness.

Fig. S5 shows the Raman spectra of GO, graphene microtube (labelled as ERGO) and chemically reduced GO (labelled as CRGO). For CRGO, the GO was reduced by hydriodic acid at 95 °C for 8 h. From Fig. S5, there are four peaks for all kinds. Peaks at 1345 cm^{-1}, 1590 cm^{-1} and 2680 cm^{-1} are assigned to the D band, G band and 2D band of carbon, respectively [25,26]. Additionally, peaks at 2420 cm^{-1} are related to the substrate. From GO to ERGO to CRGO, the intensity of the D band decreased that indicates the improved

crystalline and reduction degree, and the ratio of I_D/I_G increased that mainly means a decreased average domain size of graphene [27]. Moreover, the low intensity of 2D band for all three conditions illustrates a large number of graphene layers [28]. Furthermore, Raman spectra of graphene microtubes with different growth time are illustrated in Fig. S6. Since they have experienced nearly the same fabrication process with the same starting material, here I_D/I_G mainly stands for the reduction degree [29–31]. The I_D/I_G values for the growth time of 30 and 60 min (1.21) are larger than those for the growth time of 10 and 20 min (nearly 1.16), which reveals the inefficient reduction with increasing the growth time. This is in accordance with Figs. S1b and S4.

To study the efficiency of electrochemical reduction, i.e., the reduction result of graphene microtubes, comparison was made. Fig. 3a–c show the XPS spectra of GO, ERGO and CRGO, respectively. Here the ERGO corresponds to the growth time of 20 min. Table S2 shows the XPS atomic concentration where only C and O are observed. The concentration of O decreased from 41.3% to 11.6% after the chemical reduction, which lies in the widely accepted range of 5%–20% for reduced GO [32,33]. Moreover, the concentration of O for ERGO is decreased to 19.8%, which demonstrates a high efficiency of electrochemical reduction within a short time. The C 1s core-level XPS spectra can be decomposed by Gaussian curve fitting. In Fig. 3a for GO, peaks at 284.7 eV, 285.4 eV, 286.7 eV and 288.4 eV belong to C–C, C–O, C═O and O═C–O bonds, respectively [26,33]. After either the electrochemical reduction or the chemical reduction, peaks for C═O bond decreased and peaks for C–C bond largely increased (Fig. 3b and c). Table S3 shows the peak area fractions of bonds for GO, ERGO and CRGO. From GO to ERGO to CRGO, the increasing fraction of C–O bond is due to the increasing conversion of C═O into C–O [24,34]. Noticeably, the percentage of oxygen-containing bonds experienced an obvious drop after the electrochemical reduction. Therefore, the electrochemical technique is an effective way to reduce GO.

Furthermore, the conductivity test was used to verify the efficiency of electrochemical reduction. The conductivities of GO, ERGO and CRGO are 7.14×10^{-8}, 3.30×10^{3} and 7.97×10^{3} S m^{-1}, respectively. The conductivity of GO is increased by nearly 11 orders of magnitude after the electrochemical reduction, which illustrates its high reduction degree. Also the conductivities of ERGO and CRGO are comparable with the values of reported reduced GO [34,35]. Surprisingly, the conductivity of ERGO is independent on the bending with an angle of 50° (Fig. 4a). A deep investigation on the morphology evolution under bending was carried out (Fig. 4b and c). Little damage was found on the graphene microtube after bending for 100 times with an angle of 50° (Fig. 4b). No breakage was observed even when folding the graphene microtube (Fig. 4c). This may originate from the highly aligned graphene sheets in the tube wall, which brings about the excellent flexibility.

Since the graphene microtube possesses the excellent flexibility and conductivity, it is competent to serve as the fiber-shaped supercapacitor electrode. The specific capacitance of the graphene microtubes with different growth time is displayed in Fig. 4d. The tested current density was 0.1 A g^{-1}. At the growth time of 20 min, it has the largest specific capacitance of 135.5 F g^{-1}. The reason may be that there are more sites for absorbing the ions (coherent to Fig. 2k) and a more conductive network was formed (coherent to Fig. S7). The electrochemical properties of the graphene microtube at the growth time of 20 min were then thoroughly tested and the results are shown in Fig. 5. The CV curves are nearly rectangular at low scanning rates (Fig. 5a). The symmetric shape of the charge/discharge curves means a good coulombic efficiency, and the negligible potential drop upon discharging indicates the electrodes possess a good conductivity (Fig. 5b). The gravimetric specific capacitances are 135.5, 117.5, 109.0, and

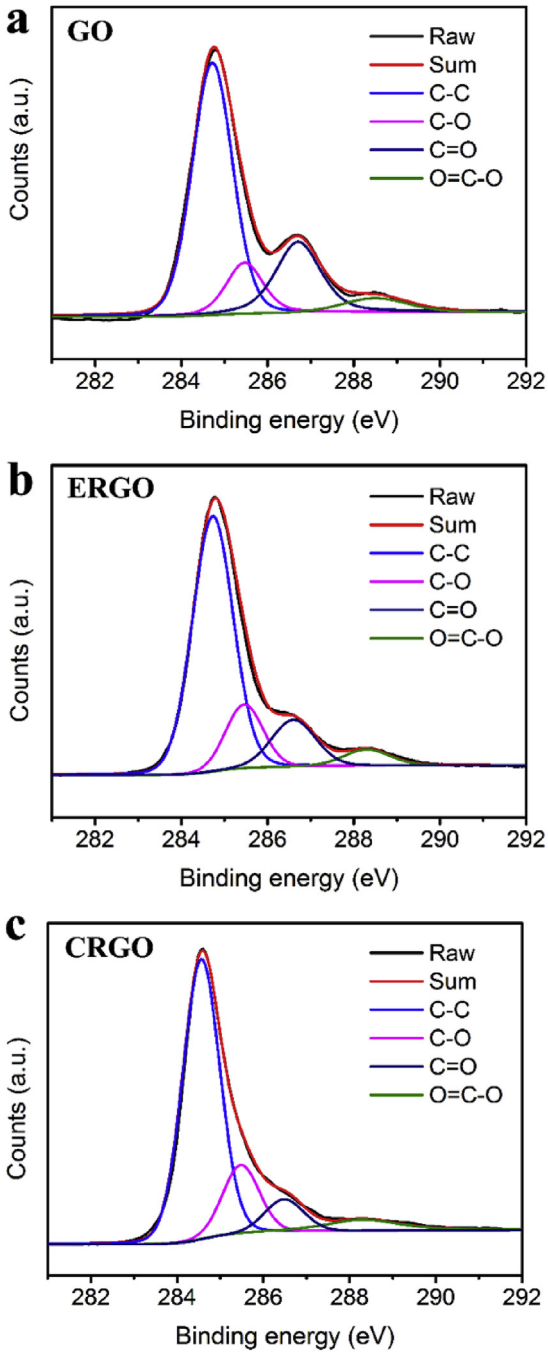

Fig. 3. XPS spectra of graphene oxides (GO) (**a**), graphene microtube (labelled as ERGO) at the growth time of 20 min (**b**) and chemically reduced GO by hydriodic acid (labelled as CRGO) (**c**). (A colour version of this figure can be viewed online.)

99.8 F g^{-1} at current densities of 0.1, 0.5, 1 and 2 A g^{-1}, respectively, which illustrates a good rate capability (Fig. 5c). Even for larger current densities, e.g., 5 and 10 A g^{-1}, the charge/discharge curves remain the symmetric shape and the specific capacitances are 85 and 56 F g^{-1}, respectively (Fig. S8a). Nearly 90% capacitance retention was achieved both after 5000 cycles at 1 A g^{-1} (Fig. 5d) and after 10000 cycles at 5 A g^{-1} (Fig. S8b), which verifies a good long-life performance.

To highlight the electrochemical performance of the proposed graphene microtube, comparisons were made. Graphene-coated Cu wire, i.e., graphene microtube with a Cu wire core (denoted as

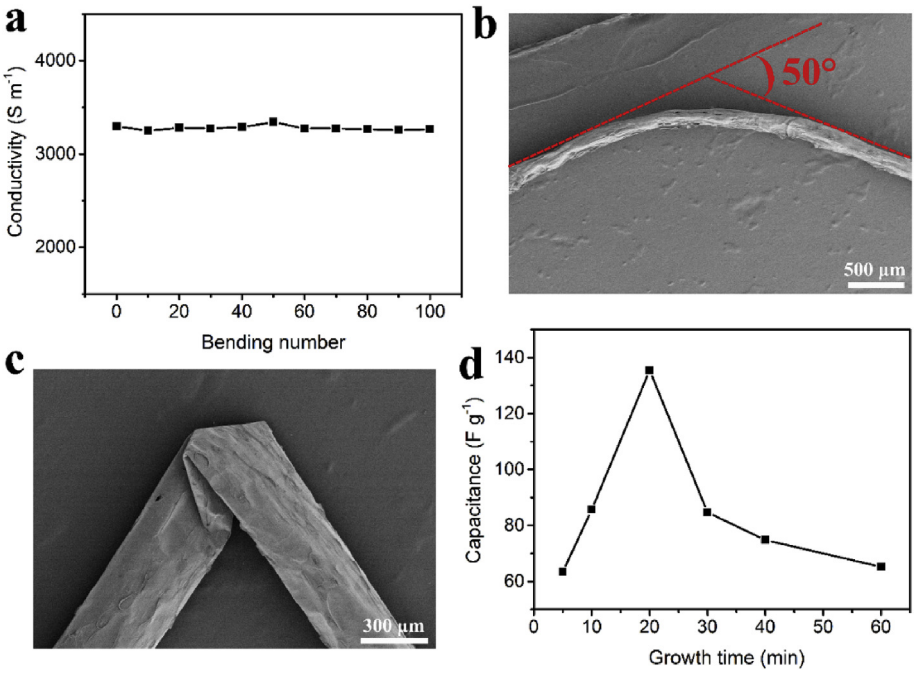

Fig. 4. Dependence of the conductivity of graphene microtube on the bending number with a bending angle of 50° (**a**). SEM morphology of the bent graphene microtube after 100 times of bending with an angle of 50° (**b**). SEM morphology of the folded graphene microtube (**c**). Dependence of the specific capacitance of the graphene microtube on the growth time (**d**). The current density was 0.1 A g^{-1}. (A colour version of this figure can be viewed online.)

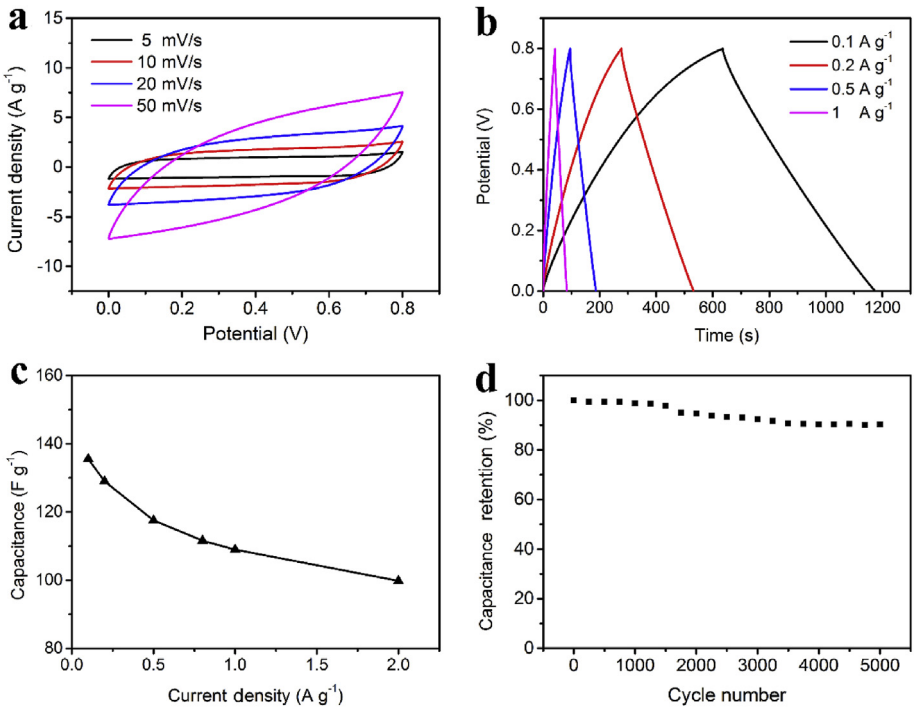

Fig. 5. Electrochemical properties of the graphene microtube at the growth time of 20 min. CV spectra (**a**), galvanostatic charge/discharge curves (**b**), rate capability (**c**) and long-life performance (**d**). (A colour version of this figure can be viewed online.)

graphene microtube@Cu wire) was shown in Fig. S9a. And graphene fiber was shown in Fig. S9b, which has a same sectional area of the graphene microtube at the growth time of 20 min (not counting the cavity). From Fig. 6a, the specific capacitance of the graphene microtube is 80% more than that of the same microtube with a Cu wire core. The main reason is the inner cavity induces additional specific capacitance [36]. Also from Fig. 6a, the specific capacitance of the graphene microtube is 2.5 times the value of the graphene fiber. This may be ascribed to the combined reasons, i.e., the inner cavity and the aligned arrangement of the graphene sheets. A sharp contrast can be observed from Fig. 2j and Fig. S6c. The graphene sheets in the graphene fiber are prone to be tangled

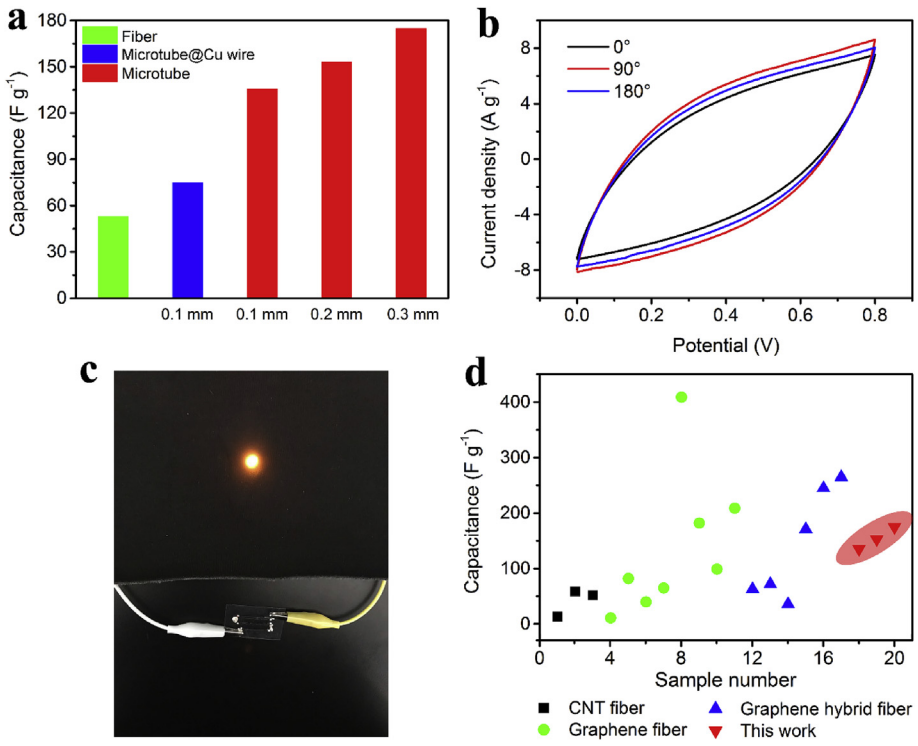

Fig. 6. Comparison on the specific capacitance between the graphene microtubes, graphene microtube@Cu wire and graphene fiber (**a**). Flexibility test of the fiber-shaped supercapacitor (**b**). A LED lightened by three fiber-shaped supercapacitors in series (**c**). Comparison on the specific capacitance between this work and other reports (data extracted from Table S4) (**d**). (A colour version of this figure can be viewed online.)

with each other. Moreover, the graphene microtubes with larger inner diameters are shown in Fig. S10, e.g., Fig. S10a produced from the Cu wire of 0.2 mm diameter (denoted as graphene microtubeΦ0.2 mm) and Fig. S10b from the Cu wire of 0.3 mm diameter (denoted as graphene microtubeΦ0.3 mm). The hollow tubular structures still complied with the Cu wires and the layer-by-layer structure of the graphene sheets remained. With increasing the inner diameter of the tube, the specific capacitance increased accordingly because of a larger inner cavity (Fig. 6a). They are 153 F g^{-1} and 175 F g^{-1} for the graphene microtubeΦ0.2 mm and graphene microtubeΦ0.3 mm, respectively.

To have a deep investigation, the specific surface area and the pore diameter distribution of the above-mentioned five samples were measured using the Brunauer–Emmett–Teller (BET) method. The nitrogen adsorption–desorption isotherm curves are shown in Fig. S11a, all of which demonstrate the IV type with a hysteresis loop, suggesting the presence of mesopores [37,38]. Correspondingly, the specific surface areas were calculated to be 55.27, 40.00, 17.35, 10.93 and 10.26 m^2 g^{-1} for graphene microtubeΦ0.3 mm, graphene microtubeΦ0.2 mm, graphene microtubeΦ0.1 mm, graphene microtube@Cu wire, and graphene fiber, respectively. Moreover, the pore size distributions are shown in Figs. S11b-S11f. It can be learned that graphene microtubes possess a narrow range of pore size distribution compared with graphene microtube@Cu wire and graphene fiber. However, for all five samples the average pore size is the same of nearly 40 nm. Therefore, the difference in the specific surface area is mainly derived from the inner cavity. These morphology results are in line with the electrochemical performance.

The flexibility of the fiber-shaped supercapacitor was also studied. The device was fixed on a PET substrate and its electrochemical performance was monitored when bending the substrate. From Fig. 6b, a good stability was confirmed even when the device was bent with an angle of 180°. Here the graphene microtube can bear a much larger bending angle (up to 180°) with the help of the gel electrolyte (Fig. S12). Also a LED is brightly lightened by three fiber-shaped supercapacitors in series (Fig. 6c). From a broad view, the proposed graphene microtube has been compared with carbon nanotube (CNT) fibers and graphene-based fibers (Table S4 and Fig. 6d). From Fig. 6d, it can be seen that the proposed graphene microtube excels the CNT fibers and most of the graphene-based fibers.

4. Conclusions

In the proposed electrochemical growth protocol, tubular structure does not collapse and graphene microtube is shape-persistent. Moreover, a high quality is achieved by an effective reduction of GO to graphene and a high regularity of layered framework of graphene sheets in the tube wall. Therefore the resulting graphene microtube presents excellent flexibility and electrochemical performance. Also, it has a big possibility to customize the shape of the graphene microtube. Consequently, the resulting graphene microtube possesses a bright prospect in gas separation, water treatment and electronics.

Acknowledgements

This work was supported by the National Natural Science Foundation of China (51603038, 51673038), Program for Innovative Research Team in University of Ministry of Education of China (IRT_16R13), Science and Technology Commission of Shanghai Municipality (16JC1400700) and the Fundamental Research Funds for the Central Universities, DHU Distinguished Young Professor Program.

Appendix A. Supplementary data

Supplementary data related to this article can be found at https://doi.org/10.1016/j.carbon.2017.10.045.

References

[1] K.S. Novoselov, A.K. Geim, S.V. Morozov, D. Jiang, Y. Zhang, S.V. Dubonos, et al., Electric field effect in atomically thin carbon films, Science 306 (5696) (2004) 666–669.

[2] C. Lee, X. Wei, J.W. Kysar, J. Hone, Measurement of the elastic properties and intrinsic strength of monolayer graphene, Science 321 (5887) (2008) 385–388.

[3] T. Kuilla, S. Bhadra, D. Yao, N.H. Kim, S. Bose, J.H. Lee, Recent advances in graphene based polymer composites, Prog. Polym. Sci. 35 (11) (2010) 1350–1375.

[4] Y. Shao, M.F. El-Kady, L.J. Wang, Q. Zhang, Y. Li, H. Wang, et al., Graphene-based materials for flexible supercapacitors, Chem. Soc. Rev. 44 (11) (2015) 3639–3665.

[5] B. Zheng, T. Huang, L. Kou, X. Zhao, K. Gopalsamy, C. Gao, Graphene fiber-based asymmetric micro-supercapacitors, J. Mater. Chem. A 2 (25) (2014) 9736–9743.

[6] J. Baringhaus, M. Ruan, F. Edler, A. Tejeda, M. Sicot, A. Taleb-Ibrahimi, et al., Exceptional ballistic transport in epitaxial graphene nanoribbons, Nature 506 (7488) (2014) 349–354.

[7] K.S. Kim, Y. Zhao, H. Jang, S.Y. Lee, J.M. Kim, K.S. Kim, et al., Large-scale pattern growth of graphene films for stretchable transparent electrodes, Nature 457 (7230) (2009) 706–710.

[8] Y. Ma, J. Zhao, L. Zhang, Y. Zhao, Q. Fan, Z. Hu, et al., The production of carbon microtubes by the carbonization of catkins and their use in the oxygen reduction reaction, Carbon 49 (15) (2011) 5292–5297.

[9] H. Yu, X. Huang, G. Wen, B. Zhong, T. Zhang, In situ synthesis of high-purity carbon microtube membrane, Mater. Lett. 65 (15) (2011) 2374–2376.

[10] M. Pfeffermann, M. Wuttke, X. Feng, A. Narita, K. Müllen, Shape-persistent graphite replica of metal wires, Adv. Mater. 29 (4) (2017), 1603732.

[11] Y. Zhao, C. Jiang, C. Hu, Z. Dong, J. Xue, Y. Meng, et al., Large-scale spinning assembly of neat, morphology-defined, graphene-based hollow fibers, ACS Nano 7 (3) (2013) 2406–2412.

[12] B. Zhang, H.-H. Wang, H. Su, L.-B. Lv, T.-J. Zhao, J.-M. Ge, et al., Nitrogen-doped graphene microtubes with opened inner voids: highly efficient metal-free electrocatalysts for alkaline hydrogen evolution reaction, Nano Res. 9 (9) (2016) 2606–2615.

[13] T. Chen, L. Dai, Macroscopic graphene fibers directly assembled from CVD-grown fiber-shaped hollow graphene tubes, Angew. Chem. Int. Ed. 127 (49) (2015) 15160–15163.

[14] D. Mendoza, Electrical conductivity of collapsed multilayer graphene tubes, World J. Nano Sci. Eng. 2 (2) (2011) 53–57.

[15] C. Hu, Y. Zhao, H. Cheng, Y. Wang, Z. Dong, C. Jiang, et al., Graphene microtubings: controlled fabrication and site-specific functionalization, Nano Lett. 12 (11) (2012) 5879–5884.

[16] J. Yu, M. Wang, P. Xu, S.-H. Cho, J. Suhr, K. Gong, et al., Ultrahigh-rate wire-shaped supercapacitor based on graphene fiber, Carbon 119 (2017) 332–338.

[17] J. Zhang, X. Yang, Y. He, Y. Bai, L. Kang, H. Xu, et al., δ-MnO_2/holey graphene hybrid fiber for all-solid-state supercapacitor, J. Mater. Chem. A 4 (23) (2016) 9088–9096.

[18] Y. Liang, Z. Wang, J. Huang, H. Cheng, F. Zhao, Y. Hu, et al., Series of in-fiber graphene supercapacitors for flexible wearable devices, J. Mater. Chem. A 3 (6) (2015) 2547–2551.

[19] S. Wang, N. Liu, J. Su, L. Li, F. Long, Z. Zou, et al., Highly stretchable and self-healable supercapacitor with reduced graphene oxide based fiber springs, ACS Nano 11 (2) (2017) 2066–2074.

[20] H. Sun, X. Fu, S. Xie, Y. Jiang, H. Peng, Electrochemical capacitors with high output voltages that mimic electric eels, Adv. Mater. 28 (10) (2016) 2070–2076.

[21] H. Cheng, Z. Dong, C. Hu, Y. Zhao, Y. Hu, L. Qu, et al., Textile electrodes woven by carbon nanotube–graphene hybrid fibers for flexible electrochemical capacitors, Nanoscale 5 (8) (2013) 3428–3434.

[22] W. Ma, S. Chen, S. Yang, W. Chen, W. Weng, Y. Cheng, et al., Flexible all-solid-state asymmetric supercapacitor based on transition metal oxide nanorods/reduced graphene oxide hybrid fibers with high energy density, Carbon 113 (2017) 151–158.

[23] S. Chen, W. Ma, Y. Cheng, Z. Weng, B. Sun, L. Wang, et al., Scalable non-liquid-crystal spinning of locally aligned graphene fibers for high-performance wearable supercapacitors, Nano Energy 15 (2015) 642–653.

[24] H.-L. Guo, X.-F. Wang, Q.-Y. Qian, F.-B. Wang, X.-H. Xia, A green approach to the synthesis of graphene nanosheets, ACS Nano 3 (9) (2009) 2653–2659.

[25] M.S. Dresselhaus, A. Jorio, M. Hofmann, G. Dresselhaus, R. Saito, Perspectives on carbon nanotubes and graphene Raman spectroscopy, Nano Lett. 10 (3) (2010) 751–758.

[26] S. Pei, H.-M. Cheng, The reduction of graphene oxide, Carbon 50 (9) (2012) 3210–3228.

[27] B. Li, L. Zhou, D. Wu, H. Peng, K. Yan, Y. Zhou, et al., Photochemical chlorination of graphene, ACS Nano 5 (7) (2011) 5957–5961.

[28] A.C. Ferrari, J. Meyer, V. Scardaci, C. Casiraghi, M. Lazzeri, F. Mauri, et al., Raman spectrum of graphene and graphene layers, Phys. Rev. Lett. 97 (18) (2006), 187401.

[29] Y. Li, K. Sheng, W. Yuan, G. Shi, A high-performance flexible fibre-shaped electrochemical capacitor based on electrochemically reduced graphene oxide, Chem. Commun. 49 (3) (2013) 291–293.

[30] A.C. Ferrari, J. Robertson, Interpretation of Raman spectra of disordered and amorphous carbon, Phys. Rev. B 61 (20) (2000) 14095–14107.

[31] I.K. Moon, J. Lee, R.S. Ruoff, H. Lee, Reduced graphene oxide by chemical graphitization, Nat. Commun. 1 (2010) 73.

[32] X.-Y. Peng, X.-X. Liu, D. Diamond, K.T. Lau, Synthesis of electrochemically-reduced graphene oxide film with controllable size and thickness and its use in supercapacitor, Carbon 49 (11) (2011) 3488–3496.

[33] Y. Shao, J. Wang, M. Engelhard, C. Wang, Y. Lin, Facile and controllable electrochemical reduction of graphene oxide and its applications, J. Mater. Chem. 20 (4) (2010) 743–748.

[34] S.Y. Toh, K.S. Loh, S.K. Kamarudin, W.R.W. Daud, Graphene production via electrochemical reduction of graphene oxide: synthesis and characterisation, Chem. Eng. J. 251 (2014) 422–434.

[35] V.B. Mohan, R. Brown, K. Jayaraman, D. Bhattacharyya, Characterisation of reduced graphene oxide: effects of reduction variables on electrical conductivity, Mater. Sci. Eng. B 193 (2015) 49–60.

[36] G. Qu, J. Cheng, X. Li, D. Yuan, P. Chen, X. Chen, et al., A fiber supercapacitor with high energy density based on hollow graphene/conducting polymer fiber electrode, Adv. Mater. 28 (19) (2016) 3646–3652.

[37] J. Hu, Z. Kang, F. Li, X. Huang, Graphene with three-dimensional architecture for high performance supercapacitor, Carbon 67 (2014) 221–229.

[38] H.-F. Ju, W.-L. Song, L.-Z. Fan, Rational design of graphene/porous carbon aerogels for high-performance flexible all-solid-state supercapacitors, J. Mater. Chem. A 2 (28) (2014) 10895–10903.